Laser Light Scattering of Poly(acrylamide) in 1 M NaCl Aqueous Solution

Qicong Ying, Guangwei Wu,† and Benjamin Chu*

Chemistry Department, State University of New York at Stony Brook, Long Island, New York 11794-3400

Ray Farinato and Logan Jackson

Cytec Industries, 1937 West Main Street, Stamford, Connecticut 06904

Received December 5, 1995; Revised Manuscript Received March 30, 1996[⊗]

ABSTRACT: Laser light scattering has been used to study the solution behavior in aqueous NaCl of poly(acrylamide) (PAM), polymerized by using two different polymerization processes: solution (S) and microemulsion (M). Results show that poly(acrylamide) samples polymerized from the microemulsion polymerization process behave as branched flexible chains, but poly(acrylamide) samples synthesized from solution polymerization exhibit a fairly expanded flexible coil−chain behavior. By combining the static light scattering results with the characteristic linewidth distribution, as determined by a Laplace inversion of the intensity−intensity time correlation function, the molecular weight distribution (MWD) and the radius of gyration distribution (RGD) could be estimated. The molecular weight dependence of the *z*-average diffusion coefficient (D_z) was determined during this conversion, with $D_z^0 = (3.05 \times 10^{-4})\ M_w^{-0.585}$ cm^2 s^{-1} and $D_z^0 = (1.52 \times 10^{-4})\ M_w^{-0.518}$ cm^2 s^{-1} for PAM(S) and PAM(M), respectively, with the weight average molecular weight M_w expressed in g mol^{-1} and D_z^0 in cm^2 s^{-1}. The superscript zero denotes the value at infinite dilution. The smaller α_D value of 0.52 for PAM(M) suggests that PAM(M) could have a fairly compact, but still soluble, flexible coil−chain structure, possibly arising as a result of (apparent) branching. Two different models, polydisperse branched chains and branched soft spheres, were used to fit the particle scattering factor obtained from SLS measurements. The results show that the particle scattering factors of samples PAM(M) (but not of PAM(S)) could be fitted satisfactorily by either model. Concentration and angular dependence of the mean characteristic linewidth, as well as the molecular weight distribution derived by using the CONTIN analysis, are presented. The origin of the apparent branching in the microemulsion prepared poly(acrylamide) is shown to be a noncovalent aggregation in 1 M NaCl which is not manifest in formamide solutions of the same polymer.

Introduction

Most poly(acrylamide) samples have high molecular weights (sometimes up to tens of millions) and high polydispersity. Poly(acrylamide) can be dissolved easily in water, enhancing the fluid viscosity considerably. Due to the enormous viscosity increase, poly(acrylamide) has been explored as a thickening agent in tertiary oil recovery. It has also been used for flocculation of colloidal particles in suspension and as a separation medium in gel electrophoresis. In 1977, Bode[1] first used a polymer physical network, i.e., non-cross-linked poly(acrylamide) in combination with agarose, for separation of proteins and double-stranded oligonucleotides. He concluded that the mechanism of sieving in linear poly(acrylamide) was similar to that occurring in cross-linked poly(acrylamide) gels. The de Gennes[2] solution theory can be used as the foundation in exploring the entangled polymer solution as a sieving medium for DNA separation.[3] Righetti and co-workers[4] demonstrated that poly(acrylamide) solutions which were made by *in situ* polymerization of acrylamide showed surprising efficiency in sieving mixtures of DNA fragments. They suggested that it might be advantageous to use *in situ* polymerization of acrylamide, as it produced a large distribution of chain lengths, which could provide a vast range of chain lengths for simultaneously sieving both short and long DNA fragments. To our knowledge, the answer for the effect of polydispersity on the separation of DNA fragments is still not clear. However, as a polymeric material, the polydispersity of poly(acrylamide) should certainly play an effective role either in the exploitation as a separation medium for DNA separation or as a thickening agent. In this work, we present laser light scattering results on the macromolecular chain behavior and polydispersity of poly(acrylamide) samples which were synthesized from different polymerization processes, solution polymerization and microemulsion polymerization. The experiments were conducted in dilute poly(acrylamide) solutions with 1 M NaCl solution as the solvent.

Experimental Section

Materials. Acrylamide (electrophoresis grade ~99%) and 2,3,3-D_3 (98%) acrylamide were purchased, respectively, from the Aldrich Chemical Co. and the Cambridge Isotope Laboratories, Inc. The surfactants Arlacel 83 and Atlas G-1086 were obtained from the Ruger Chemical Co., Division of ICI Inc. The paraffin oil, LPA-170, was obtained from the Vista Chemical Co. 2-Propanol (IPA) was purchased from the J. T. Baker Co., and V-44 was obtained from the Wako Chemical Co. All of the above chemicals were used as obtained.

A Blak-Ray long wave ultraviolet lamp, Model B 100 AP, was used as a UV light source for the polymerizations. All reactions were carried out in a well-ventilated fume hood.

PAM Microemulsion Preparation. The polymerizations were carried out, using both the H-acrylamide and 2,3,3-D_3-acrylamide, in a manner similar to that described elsewhere.[5,6] The polymers were denoted as PAM(HM) and PAM(DM), respectively.

Oil phases were made, on a small scale, by preparing a stock solution of oil and surfactants (w/w) and placing the desired amount into a 5 dram sample vial. The aqueous phase was prepared in a separate vessel by addition of acrylamide (AMD),

* Author to whom correspondence should be addressed.
† Present address: Department of Chemical Engineering, Princeton University.
⊗ Abstract published in *Advance ACS Abstracts,* May 15, 1996.

S0024-9297(95)01798-0 CCC: $12.00

water, and a stock deionized water solution containing V-44. The aqueous phase was added to the oil phase with stirring.

The reactor was then sealed with a rubber septum, and the monomer microemulsion was sparged with nitrogen (100 mL/min, 30 min). A small thermocouple was inserted through the septum to monitor the polymerization temperature. After the initial nitrogen sparge, UV light was introduced, and the reactions were allowed to proceed slowly without external cooling for 60 min. The resulting microemulsions were clear, thermodynamically stable, low viscosity fluids.

The polymer was precipitated from the microemulsion by dilution of the emulsion (6.0 g) into hexane (25.0 g). The hexane solution was then added slowly to vigorously stirred acetone (500 g). The precipitated polymer was filtered and returned to acetone (100 g) and allowed to stir for 16 h to extract any residual oil and surfactant. The resulting polymer was filtered and then dried under vacuum for 48 h.

PAM Solution Polymerization. Both the H-acrylamide and 2,3,3-D_3-acrylamide solution polymers, denoted as PAM(HS) and PAM(DS), respectively, were prepared by the following procedure.

Acrylamide (1.000 g) and water (19.000 g) containing 2-propanol (0.020 g) and V-44 (0.0005 g) were placed in a 5 dram sample vial. The reactor was sealed with a rubber septum and sparged with nitrogen (100 mL/min, 30 min). A small thermocouple was inserted to monitor polymerization temperature. After the initial nitrogen sparge, the nitrogen was continued, the inlet was raised above the fluid level, and UV light was introduced. The reactions were allowed to proceed without external cooling for 90 min. Clear, viscous fluids were obtained. The fluids were used in these studies as prepared.

Solution Preparation for Light Scattering Measurements. Solutions were prepared by the weighing method. Two stock solutions with concentrations of 6.980×10^{-4} and 6.754×10^{-4} g/mL in 1 M NaCl aqueous solution for PAM(HS) and PAM(DS), respectively, were directly prepared from the solution samples. The stock solution was kept in a 50 mL volumetric flask, which was rotated using a slow speed motor to make the stock solution uniform. After having stirred for 4 days, the uniform stock solution was diluted to the designated concentrations. Stock solutions with concentrations of 5.160×10^{-4} and 5.480×10^{-4} g/mL for PAM(HM) and PAM(DM) in 1 M NaCl aqueous solution, respectively, were prepared from the dry samples. After having mixed the dry sample with the solvent, the stock solution was kept in a 40 °C thermoblock for at least 4−6 days, and then the stock solution was stirred slowly by rotating the volumetric flask at a slow speed for at least another 4−5 days. With the expected high molecular weight ($>1 \times 10^6$ g mol^{-1}) of these samples, it took at least 10 days to make a uniform solution. Again, the uniform stock solution was diluted to the designated concentrations. Each diluted solution for light scattering measurement was clarified by centrifugation for 6 h at $(7.7 \times 10^3)g$ (~8000 rpm). The upper dust-free solution was transferred into a dust-free light scattering cell by a dust-free pipet. For each PAM sample, four solutions of different concentrations were prepared for light scattering measurements.

For the experiments designed to compare the behavior of PAM(HM) in 1 M NaCl and in formamide, the dried precipitated polymer was dissolved overnight by gently rolling a 0.1 wt % sample in solvent prefiltered through a 0.2 μm Anotop filter (Alltech Inc., Deerfield, IL). As a control, a commercial sample of a high molecular weight poly(acrylamide) from Scientific Polymer Products, PAM(SPP001), was also run. For aqueous solutions, water from a MilliQ purification system was used, and the NaCl was added to the stock polymer solution the next day. For the formamide solutions, prefiltered chromatography grade formamide (Aldrich) was used. The samples were clarified using centrifugation: 4 h at 15 000 rpm in a Sorvall RC2-B with a fixed angle rotor (SS-34). This corresponded to approximately 18000g at the average solution depth. The upper portions of the clarified solutions were gravity siphoned through a closed system directly into the scattering cell.

Light Scattering Measurements. A laboratory-built laser light scattering spectrometer operating at a wavelength of 514.5 nm with an output power of ~600 mW was used to perform static light scattering (SLS) and dynamic light scattering (DLS) measurements at scattering angles between 15° and 135° and temperature $T = 25$ °C.[7] The intensity autocorrelation function was determined at scattering angles 33°, 45°, 60°, and 90° with a Brookhaven Instruments BI-9000 digital correlator. The measured intensity autocorrelation function was accepted only if the difference between the measured and the calculated baselines was less than 0.1%.

For the experiments designed to compare the behavior of PAM(HM) in 1 M NaCl and in formamide, a DAWN light scattering photometer (Wyatt Technology, Santa Barbara, CA) was used in the flow mode to measure the intensity light scattering at multiple angles typically in the range of 23−150° with an incident wavelength of $\lambda_0 = 632.8$ nm. Toluene was used as a reference for calculating the excess Rayleigh ratio, R_{ex}.

A Brookhaven Instruments (Holtsville, NY) BI-200SM goniometer and a BI-9000 correlator were used to measure the intensity−intensity autocorrelation functions for vertically polarized $\lambda_0 = 488$ nm light (Spectra Physics 2017-05S Ar^+ ion laser; ~400 mW) scattered from clarified dilute (65 μg/mL) solutions of the PAM(HM) and PAM(SPP001) over the angular range 25−75°. The average relaxation rates were computed using a second-order cumulants analysis. The z-average equivalent sphere hydrodynamic diameters, $\langle d_H \rangle_z$, from the second cumulants analysis were extrapolated to $\theta = 0°$ on plots of $1/\langle d_H \rangle_z$ vs $\sin^2(\theta/2)$.

Results and Discussion

In order to investigate the possible sources of the apparent nonlinear chain behavior in 1 M NaCl of the poly(acrylamides) prepared in the microemulsion formulations, we measured the light scattered from PAM(HM) in formamide. This solvent was chosen on the basis of work done in Kulicke's group[8] on slow changes in the aqueous solution structure of poly(acrylamide). They ascribed these changes to intramolecular H-bond rearrangements and found that such behavior did not occur in formamide.[8] This prompted us to try dissociating any noncovalent structures in the PAM(HM) by dissolving it in formamide. As a control, we compared the light scattering from a linear high molecular weight poly(acrylamide), PAM(SP001), both in 1 M NaCl and in formamide.

SLS Measurements. For vertically polarized incident light and polydisperse macromolecules with weight average molecular weight M_w (g mol^{-1}) and concentration C (g/mL), the excess Rayleigh ratio R_{ex} can be expressed as

$$\frac{HC}{R_{ex}} \simeq \frac{1}{M_w P(q)} + 2A_2 C \qquad (1)$$

where $R_{ex} = (I_s - I_0) r_d^2 / I^0$ with I_s being the solution scattered intensity; I_0, the solvent scattered intensity; r_d, the detector distance from the scattering center; and I^0, the incident intensity. $H = (4\pi^2 n_0^2 / \lambda_0^4 N_A)(\partial n/\partial C)_T^2$ (mol cm^2 g^{-2}) is the optical constant, with n_0, λ_0, N_A, and $(\partial n/\partial C)_T$ being the solvent refractive index, the incident wavelength *in vacuo*, Avogadro's number, and the specific refractive index increment at temperature T, respectively. $P(q)$ is the particle scattering factor, and $q[=(4\pi n/\lambda_0) \sin(\theta/2)]$ is the magnitude of the momentum transfer vector. A_2 (mol g^{-2} cm^3) denotes the second virial coefficient. At sufficiently dilute concentrations, $P(q)^{-1}(C \to 0) = (1 + q^2 R_g^2/3)$, and the z-average radius of gyration R_g can be evaluated. At small scattering angles $P(q \to 0) = 1$, M_w is determined from

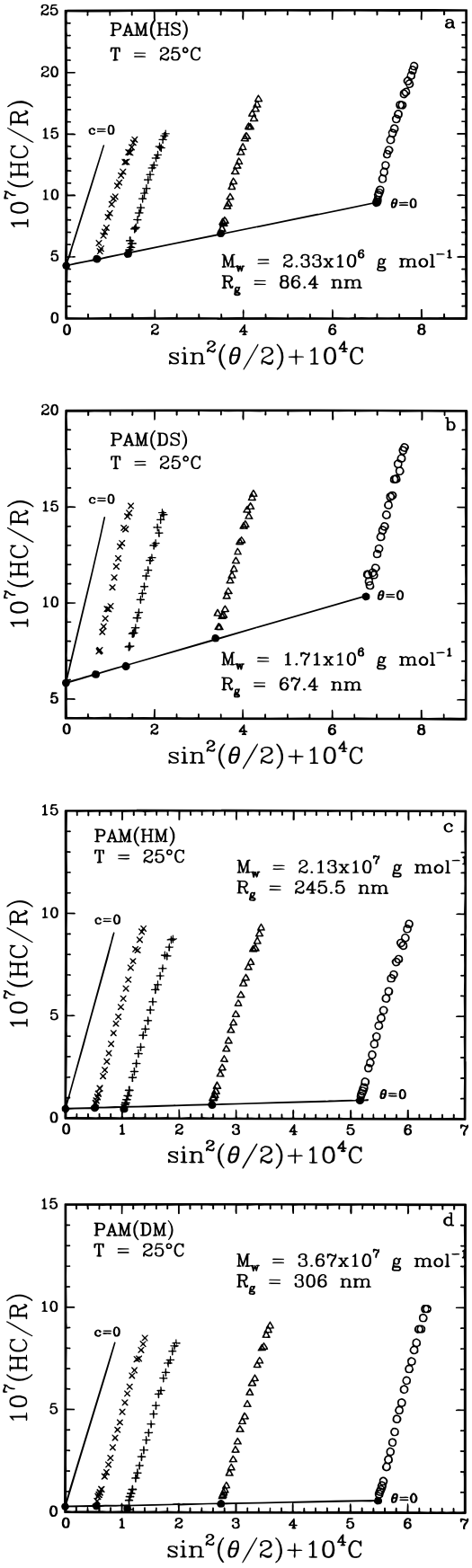

Figure 1. Zimm plots of PAM in 1 M NaCl aqueous solution at 25 °C. (a) PAM(HS); (b) PAM(DS); (c) PAM(HM); (d) PAM(DM).

eq 1, if H is known. In the present work, $H = 3.80 \times 10^{-7}$ mol cm^2 g^{-2} was obtained with $(\partial n/\partial C) \simeq 0.15$ and $n_0 = 1.34$, which was determined at $\lambda_0 = 589$ nm.[9] We accepted this value in computing H, because the difference in wavelength between the sodium light and the laser wavelength ($\lambda_0 = 514.5$ nm) used in this work was fairly small to effect the numerical value for H. The value of $(\partial n/\partial C) \simeq 0.15$ for PAM in a 1 M NaCl aqueous solution at 25 °C was estimated from $(\partial n/\partial C) = (1/\rho)(n_2 - n_0)$ with $\rho \sim 1.1$ and $n_2 \sim 1.5$, where ρ and n_2 are the density and refractive index of PAM, respectively. We also assumed that the difference in density and in refractive index between the hydrogenated poly(acrylamide) and the deuterated poly(acrylamide) could be neglected. The estimated values of ρ and n_2 used in this work could introduce a few percent uncertainties in the absolute value of the molecular weight of PAM, but it would not have an influence on the dilute solution behavior of poly(acrylamide).

Table 1. Static and Dynamic Properties of PAM in 1 M NaCl Aqueous Solution

sample	PAM(HS)	PAM(DS)	PAM(HM)	PAM(DM)
$M_w/10^6$ g mol^{-1}	2.33	1.71	21.3	36.7
R_g/nm	86.4	67.4	246	306[a]
$A_2/10^{-4}$ mol g^{-2} cm^3	3.66	3.14	0.43	0.29
$D_z^0/10^{-8}$ cm^2 s^{-1}	5.05	6.30	1.22	0.90
R_h/nm	39.5	31.7	163	190
R_g/R_h	2.2	2.1	1.5	1.6

[a] At 15° scattering angle, $q \simeq 4.3 \times 10^{-3}$ nm^{-1}. Thus, for PAM(DM) $qR_g \simeq 1.3 > 1$, suggesting that the value of R_g could be slightly off. However, from the Berry plots in Figure 4, the curvature appears reasonable with no sharp drops at small scattering angles, except for one point in Figure 4b for PAM(DM).

For the calculation of the excess Rayleigh ratio, benzene was used as a reference standard. A correction for the difference in the refractive index between benzene and the solvent was $(n_0/n_B)^2$, with n_B being the benzene refractive index at $\lambda_0 = 514.5$ nm. Then, $R_{ex} = [(I_s - I_0)/I^0](n_0/n_B)^2 R_{vv,B}$, where $R_{vv,B}$ denotes the Rayleigh ratio of benzene for vertically polarized incident and scattered light. From the wavelength dependence of the Rayleigh ratio of benzene and the depolarization ratio of benzene at 25 °C,[10] we found $R_{vv,B} = 24.2 \times 10^{-6}$ cm^{-1} at $\lambda_0 = 514.5$ nm and 25 °C.

Panels a, b, c, and d of Figure 1 show static Zimm plots of four PAM samples. The values of M_w, R_g, and A_2 are listed in Table 1. The results show that these poly(acrylamide) samples have very high molecular weights, especially for PAM(HM) and PAM(DM) samples which were polymerized in a microemulsion process. The values of M_w were at least 1 order of magnitude higher than those of PAM(HS) and PAM(DS) synthesized from the solution polymerization process due to the use of a chain transfer agent in the solution polymerization. The molecular weight dependence of A_2, as shown in Figure 2, deviates from the scaling concept prediction, i.e., $A_2 \sim N^{-\alpha_v}$ and $\alpha_v = {}^1/_5$ (dashed line in Figure 2), where N is the degree of polymerization of a polymer chain.[11] Nevertheless, it is well-known that in the high molecular weight region the value of the exponent α_v could be larger than 0.2. The deviation of α_v from 0.20 could, therefore, arise simply as a result of very high molecular weight and high polydispersity of PAM samples. α_v could be greater than 0.2 for star or highly branched chain polymers.[12,13] Therefore, the possibility that the microemulsion samples of PAM might behave as branched-chain macromolecules should also be considered.

Burchard[14] presented a polydisperse branched chain model for describing the dilute solution behavior of a

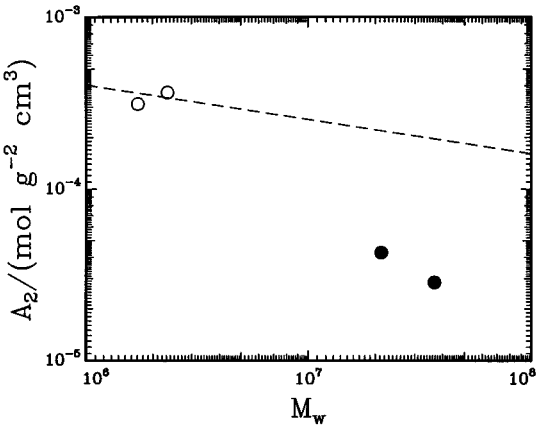

Figure 2. Plot of A_2 versus molecular weight for the four PAM samples. Hollow circles: PAM(S); full circles: PAM(M). The dashed line is drawn by using the equation $A_2 = (6.4 \times 10^{-3})M_w^{-0.2}$.

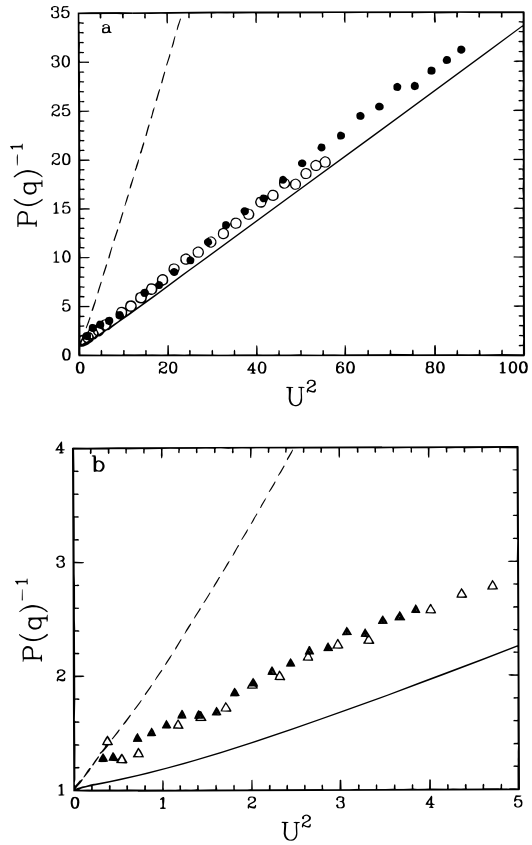

Figure 3. Reciprocal particle-scattering factor of star molecules with polydisperse rays, where f denotes the number of rays per molecule; solid line, $f = 1$; dashed line, $f = 2$. In comparison with experimental data of PAM samples. (a) Hollow circles: PAM(HM); full circles: PAM(DM); (b) hollow triangles: PAM(HS); full triangles: PAM(DS).

branched molecule with polydisperse rays. If the polydisperse rays could be described by a Schulz−Flory distribution, the particle scattering factor $P(q)$ is then given by

$$P(q) = \frac{1 + U^2/(3f)}{[1 + U^2(f+1)/(6f)]^2} \tag{2}$$

where $U^2 = q^2R_g^2$ and f is the number of rays. According to the theory, the case $f = 1$ corresponds to linear chains and randomly branched f-functional polycondensates. A comparison of this model with experimental data of samples PAM(HM) and PAM(DM), as shown in Figure 3a, indicates that the chain behavior of those samples could be satisfactorily described by a branched chain-with the polydisperse rays model having $1 \leq$ average $f < 2$. In Figure 3b, the theoretical fitting curves are compared with experimental data of PAM(HS) and PAM(DS). On close examination, the data points show a slight concave downward tendency. With $M_w/M_n \gg 2$, the plot of $P(q)^{-1}$ versus U^2 could concave downward. Thus, a definite criterion for branching is absent according to Figure 3b, because the high degree of polydispersity could block the branching effect, especially when the branching behavior is not explicit.[14]

The experimental data are also compared with a soft-sphere model[15] for a regularly branched flexible chain, which may have n shells, and each branched chain connecting adjacent shells may have m repeating units with

$$m = \frac{N-1}{3x} \tag{3}$$

where N and x denote the degree of polymerization of the total molecule and the number of chains belonging to one of the three branches of the trifunctional centrosymmetric branching unit, respectively. The particle structure factor is then given by

$$P(q) = (1/N^2)\{1 + 6P_1P_2 + 6x[P_0 + (P_1P_2)^2] + 3P_1{}^2P_6[3x - P_2 + (x+1)(P_5P_2 - P_3P_4)]\} \tag{4}$$

with

$$P_0 = (1/y^4)[my^2 - (1 - \phi^m)]$$

$$P_1 = \phi(1 - \phi^m)/(1 - \phi)$$

$$P_2 = [1 - (2\phi^m)^n]/(1 - 2\phi^m)$$

$$P_3 = (1 - \phi^{2mn})/(1 - \phi^m)$$

$$P_4 = (1 - \phi^{2mn})/(1 - 2\phi^{2m})$$

$$P_5 = \phi^{m(n+1)}/(1 - 2\phi^{2m})$$

$$P_6 = 1/(1 - 2\phi^m)$$

where $\phi = \exp(-y^2)$, $y^2 = (b^2q^2)/6$ with b being the effective bond length of the repeating units.

The mean-square radius of gyration $R_g{}^2$ then has the form

$$R_g{}^2 = b^2(3m^3/2N^2)\{x(^1/_3 + 10n - 6) + 6x^2(n-2) + 4n + [2(x+1)n - 3x]/m\} \tag{5}$$

Panels a and b of Figure 4 show the Berry plots of the reciprocal particle scattering factor of the soft-sphere model in comparison with the experimental data of PAM(HM) and PAM(DM), respectively. The parameters used in plotting the theoretical curves are listed in Table 2. The value chosen for b is to ensure that, (1) in the Berry plot, the theoretical curve fits the data points and (2) the theoretically calculated value of $R_{g,cal}$ (from eq 5) should be in agreement with the R_g value determined by SLS. We let $y^2 = (b^{*2}q^2)/6$, where b^* is the effective

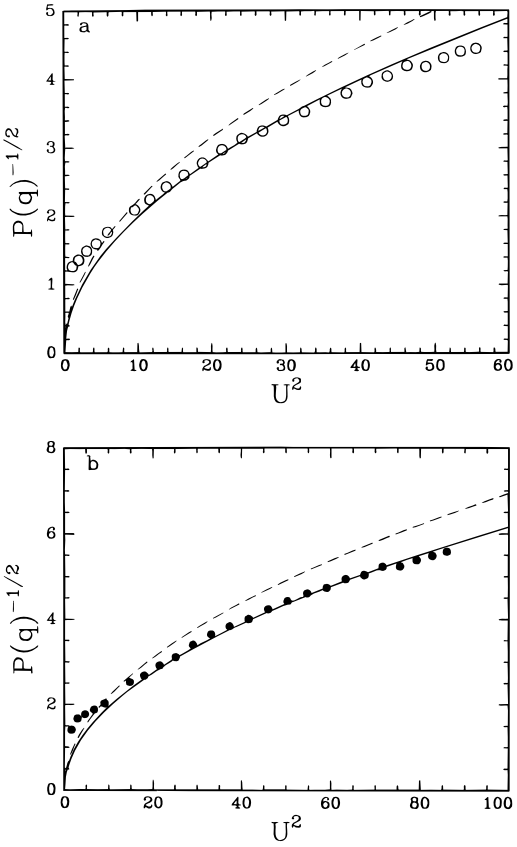

Figure 4. Berry plots of the reciprocal particle-scattering factor of the soft-sphere model. Solid line: $n = 1$; dashed line: $n = 2$. In comparison with experimental data of PAM-(M) samples. (a) Hollow circles: PAM(HM); (b) full circles: PAM(DM).

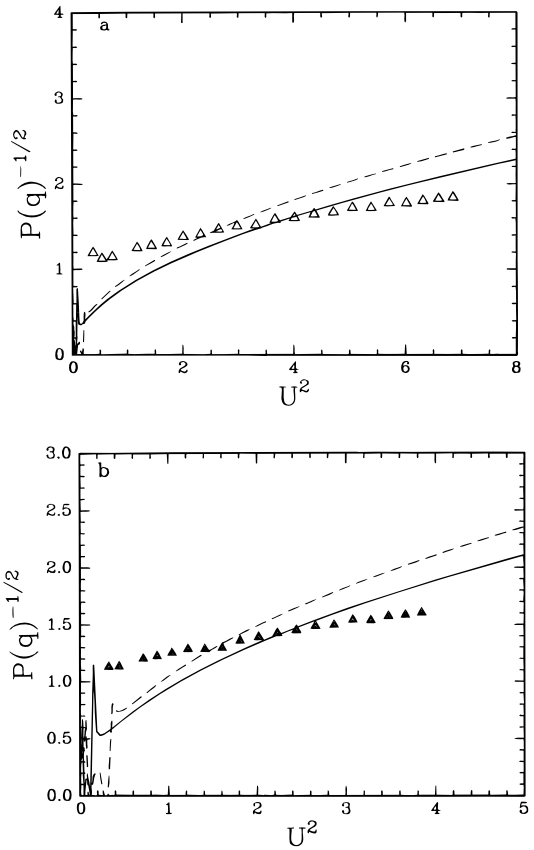

Figure 5. Berry plots of the reciprocal particle-scattering factor of the soft-sphere model. Solid line: $n = 1$; dashed line: $n = 2$. In comparison with experimental data of PAM-(S) samples. (a) Hollow triangles: PAM(HS); (b) full triangles: PAM(DS).

Table 2. Parameters Used in Berry Plots of the Reciprocal Particle Scattering Factor for the Soft-Sphere Model

sample	PAM(HM)	PAM(DM)	sample	PAM(HM)	PAM(DM)
$N/10^5$	3.0	5.2	b^*/nm	6.3	5.9
n	1	1	b/nm	1.3	1.2
x	1	1	$R_{g,cal}$[a]/nm	240	316
$m/10^5$	1.0	1.7			

[a] Calculated from eq 5.

segment length. Then, $b^* = \nu b$, with ν being a proportional constant, which should depend only on the polymer chain rigidity. The best fitting results for PAM-(HM) and PAM(DM) with $n = 1$, as shown in Figure 4a,b, give the b^* values of 6.3 and 5.9 nm, respectively. With the average value of $b^* = 6.1$ nm, the values of $R_{g,cal}$ for both PAM(HM) and PAM(DM) are in fairly good agreement with the experimental results with an error of ±3%, while $\nu = 5$, as listed in Table 2. The fitting results for PAM(HS) and PAM(DS) are shown in Figure 5, panels a and b, respectively. Obviously, the soft-sphere model could not be used to portray the chain geometry of PAM(HS) and PAM(DS). The fitting results by using either a polydisperse branched chain model or a soft-sphere model reveal the difference of chain geometry between PAM(M) prepared by using the microemulsion process and PAM(S) synthesized by using the solution polymerization process. PAM(HM) and PAM(DM) form more compact coils made of possibly branched chains, while PAM(HS) and PAM(DS) display the chain behavior in a more expanded flexible chain conformation. The same conclusions can be drawn if we were to use Zimm plots instead of Berry plots. It is also noted that the theoretical model (e.g., Figure 5) has problems at small values of U.

The Mark−Houwink exponent α_η could be calculated from $\alpha_\eta = 3\alpha_D - 1$, where α_D denotes the exponent in $\langle D \rangle_z = k_D M^{-\alpha_D}$. The values of α_η for PAM(S) and PAM-(M) were found to be 0.76 and 0.55, respectively. It is well-known that the value of the Mark−Houwink exponent is implicated in the conformation of a macromolecular chain. According to the Flory theory, if the chain coil is fairly compact as a nondraining chain $\alpha_\eta = 0.5$, while for a looser coil, $\alpha_\eta \sim 0.75$. In comparing a branching chain with a linear chain of the same molecular weight, the segment distribution of a branched chain is more compact than that of a linear chain, and the α_η value could then be smaller than that of a linear chain and be close to the limiting value of 0.5. Therefore, based on the theoretical estimation, the α_η value of 0.55 for PAM(M) could be used as additional evidence for the existence of branching chain structures. On the other hand, a value of 0.76 for α_η of PAM(S) suggests an expanded linear coil conformation for poly(acrylamide) prepared by the solution polymerization process.

For the experiments designed to compare the behavior of PAM(HM) in 1 M NaCl and in formamide, the light scattering data at 4−6 concentrations (C) were analyzed according to both the double extrapolation method of Zimm (HC/R_{ex} vs $\sin^2(\theta/2) + kC$) and a method involving the intensity directly (R_{ex}/HC vs $\sin^2(\theta/2) + kC$), which is referred to as a Debye plot in the Wyatt Technology software. Both of these methods yielded M_w values within experimental error of each other. However, a smaller angular range of data had to be used for the

Table 3. Comparison of PAM Solution Properties in 1 M NaCl and in Formamide

	PAM(HM) (1 M NaCl)	PAM(HM) (formamide)	PAM(SP001) (1 M NaCl)	PAM(SPP001) (formamide)
$M_w/10^6$ g mol^{-1}	26.5 ± 2	6.3 ± 0.2	3.9 ± 0.1	4.1 ± 0.2
R_g/nm	270 ± 7	172 ± 4	175 ± 2	178 ± 4
$A_2/10^{-4}$ mol g^{-2} cm^3	0.81	1.3	2.7	4.0
R_h/nm	176	93	84	72
R_g/R_h	1.5	1.8	2.1	2.5

Debye plot in order to allow for a reasonable polynomial fit (third order in $\sin^2(\theta/2)$ for the PAM(HM) and second order for the PAM(SP001)). The results reported in Table 3 are based on the Zimm analysis and are in reasonable agreement with measurements made with the other experimental apparatus (Table 1) for the 1 M NaCl solutions. The $\partial n/\partial C$ values used, 0.175 cm^3/g for 1 M NaCl and 0.110 cm^3/g for formamide, were taken from literature.[16−18] The R_g, M_w parameters for the PAM(SP001) in 1 M NaCl agree well with literature data on linear poly(acrylamide),[16] whereas the R_g of PAM(HM) in 1 M NaCl is somewhat smaller than expected based on its M_w.

DLS Measurements. The measured unnormalized intensity autocorrelation function $G^{(2)}(\tau)$ has the form

$$G^{(2)}(\tau) = A[1 + \beta|g^{(1)}(\tau)|^2] \tag{6}$$

with τ being the delay time, A the baseline, β a spatial coherence factor, and $g^{(1)}(\tau)$ the first-order normalized electric field correlation function, which is related to the normalized characteristic linewidth distribution function $G(\Gamma)$ by the Laplace integral equation.

$$g^{(1)}(\tau) = \int G(\Gamma) \exp(-\Gamma\tau)\, d\Gamma \tag{7}$$

The correlation data were analyzed by using the method of cumulants[19,20] and the CONTIN method,[21] yielding a mean linewidth $\bar{\Gamma}$ and the variance $\mu_2/\bar{\Gamma}^2$, with

$$\bar{\Gamma} = \int \Gamma\, G(\Gamma)\, d\Gamma \tag{8}$$

and

$$\mu_2 = \int (\Gamma - \bar{\Gamma})^2\, G(\Gamma)\, d\Gamma \tag{9}$$

In the limit of low q ($q \to 0$ or $qR_g < 1$), the mean characteristic linewidth $\bar{\Gamma}$ is related to the z-average translational diffusion coefficient D_z by the relation

$$\lim_{q\to 0} \bar{\Gamma} = D_z q^2 \tag{10}$$

The concentration effect can be represented by a second virial coefficient expansion

$$D_z = D_z^0(1 + k_d C) \tag{11}$$

where the superscript zero denotes the value at infinite dilution ($c \to 0$) and k_d is the diffusion second virial coefficient. At finite scattering angles, the characteristic linewidth contains information on internal motions of the polymer as well as its translational motions. Equation 10 is no longer valid at $qR_g \gg 1$, but can be modified to yield

$$\bar{\Gamma}/q^2 \simeq D_z(1 + f_c\langle R_g^2\rangle q^2) \tag{12}$$

where f_c is a dimensionless number and depends on chain structure, polydispersity, and solvent quality.[22] The theoretical f_c value of regular stars or polydisperse stars was predicted to be in the range of 0.1−0.2; but it could also be in the range of 0.04−0.17 in the preaverage approximation. The polydispersity effect causes an increase in the coefficient f_c, and the branching effect causes a decrease in f_c, but the effects could be highly overestimated in the preaverage approximation. In this work, we found that PAM(DM) and PAM(HM) have low f_c values, with $f_c = 0.05$ and 0.08, respectively, while PAM(DS) and PAM(HS) have higher f_c values, with $f_c = 0.11$ and 0.12, respectively. As the PAM samples studied have very broad MWD with $M_z/M_w \sim 5$, as shown in Table 4, and high M_w, the magnitude of f_c could not be used to distinguish chain structures even in a qualitative manner.

Table 4. Comparison of Experimental Results and Parameters Used in MWD and RGD Calculation

sample	PAM(HS)	PAM(DS)	PAM(HM)	PAM(DM)
α_D	0.585		0.518	
$k_D/10^{-4}$	3.05		1.52	
$M_{w,fit}/10^6$	2.27	1.77	23.1	34.5
$M_w/10^6$	2.33	1.71	21.3	36.7
$M_z/10^6$	12.8	7.6	10.2	151
M_z/M_w	5.6	4.3	4.4	4.4
$k_g/10^{-3}$	7.90		19.6	
$R_{g,fit}$/nm	90.8	66.5	245	313
R_g/nm	86.4	67.4	246	306

The average hydrodynamic radius R_h can be calculated by using the Stokes−Einstein relation:

$$R_h = k_B T/(6\pi\eta D) \tag{13}$$

where k_B, T, and η are the Boltzmann constant, the temperature (K), and the solvent viscosity in P, respectively. In Table 1, the experimental values of R_g, R_h, and the ratio of R_g/R_h are listed. The ratio of R_g/R_h for PAM(HS) and PAM(DS) has a value of ∼2.2. It is fairly close to the theoretical value 2, which was calculated from a polydisperse coil in a good solvent. The ratio of R_g/R_h for PAM(HM) and PAM(DM) has a value of ∼1.6, which is in the R_g/R_h range of a star polymer ($R_g/R_h \sim$ 1.1−1.7).[23] However, these results also exhibit that PAM samples prepared by using a microemulsion process have a more compact chain conformation than that prepared from solution polymerization.

In the CONTIN method, one can analyze the data by using either Γ or τ ($\equiv\Gamma^{-1}$) as the variable. The results are weighted differently, resulting in slightly different numerical values of R_h. The molecular weight distributions (MWD) based on the diffusion coefficient distribution (or Γ distribution) for PAM(S) and PAM(M) were evaluated by using the CONTIN method and the relationship of $D_z = k_D M^{-\alpha_D}$, if k_D and α_D are known. The radius of gyration distribution can also be calculated from the molecular weight distribution by using the relation of $R_g = k_g M^{\alpha_g}$ with known constants k_g and α_g.

At infinite dilution, in plots of $F(q,\Gamma)$ versus $\Gamma_{i,q}$ at different scattering angles, the transformation to MWD can be achieved by considering a transform of $F(q,\Gamma)$ to representative weight fractions w_i (or $(w\Gamma)_i$) along the y-axis, and of $\Gamma_{i,q}$ to molecular weight M_i along the x-axis. A plot of $F(w\Gamma)$ vs Γ for PAM(DM), evaluated

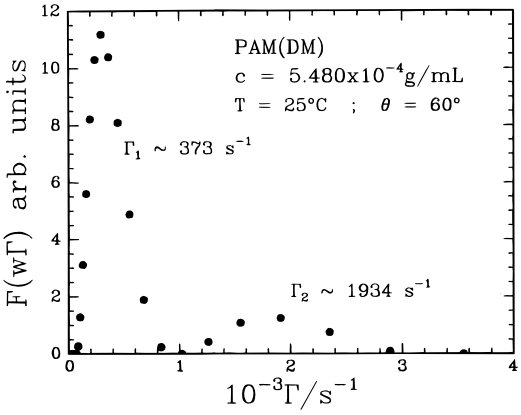

Figure 6. Plot of $F(w\Gamma)$ versus Γ for sample PAM(DM) measured at 25 °C and scattering angle $\theta = 60°$.

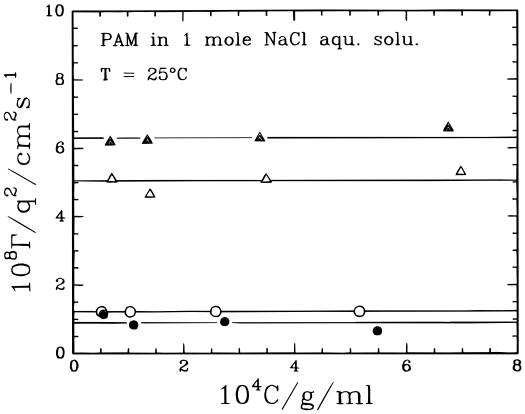

Figure 7. Plot of concentration dependence of $\bar{\Gamma}/q^2$ of PAM in 1 M NaCl aqueous solution at 25 °C. Hollow circles: PAM-(HM); full circles: PAM(DM); hollow triangles: PAM(HS); full triangles: PAM(DS).

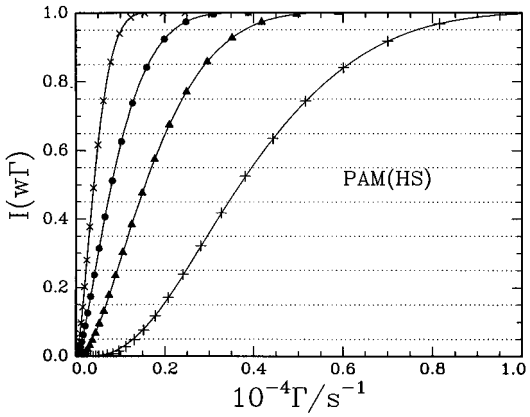

Figure 8. Plot of integral distribution curves $I(w\Gamma)_q$ versus Γ of PAM(HS) measured at different q. Crosses: $q = 9.32 \times 10^4$ cm^{-1}; full circles: $q = 1.26 \times 10^5$ cm^{-1}; full triangles: $q = 1.64 \times 10^5$ cm^{-1}; pluses: $q = 2.32 \times 10^5$ cm^{-1}.

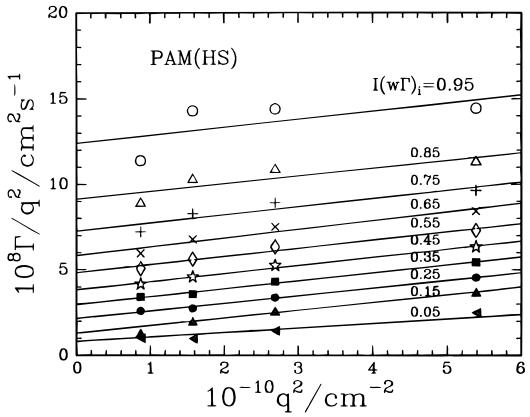

Figure 9. Plot of q^2 dependence of $\bar{\Gamma}/q^2$ of representative fractions, $I(w\Gamma)_{i=0.05,...0.95}$, of PAM(HM).

by using the CONTIN program, is shown in Figure 6. The procedure used for the transformation of the $F(q,\Gamma)$ plot to MWD can be described as follows.

(a) The DLS measurements for PAM samples were conducted at four different concentrations. In the solution concentration range ($c < 8 \times 10^{-4}$ g/mL), the concentration dependence of $\bar{\Gamma}/q^2$ for the four PAM samples could be neglected, as shown in Figure 7. Therefore, in the transformation process only the q dependence of Γ/q^2 should be considered. By using a computer integral program, a normalized integral curve of $I(w\Gamma)$ vs Γ was obtained as shown in Figure 8, from which the representative weight fractions $I(w\Gamma)_{i,q}$ were easily determined. For example, we chose ten representative fractions $I(w\Gamma)_{i,q}$ of PAM(HS) determined at different q, with $i = 0.05$, 0.15, 0.25, 0.35, 0.45, 0.55, 0.65, 0.75, 0.85, and 0.95, which are denoted by the dotted lines in Figure 8 (for better curve plot more than ten representative fractions could be chosen). The $\Gamma_{i,q}$ values corresponding to each representative fraction ($I(w\Gamma)_i$) at different q could be evaluated simply from the x-axis of the integral curves. By means of eq 12, the q dependence of $\bar{\Gamma}_{i,q}/q^2$ for representative fractions $I(w\Gamma)_i$, where $i = 0.05$, 0.1, ... 0.95, are plotted in Figure 9, and the integral distribution of translational diffusion coefficient could be determined from $(\Gamma_i/q^2)_{q\to 0,c\to 0,i=0.05...0.95}$.

(b) The transform of distribution of translational diffusion coefficient to MWD is based on the relationship of $D_z = k_D M^{-\alpha_D}$. In our analysis, the values of M_w of four samples were determined by SLS. The value of D_z, as an initial approximation, could be estimated from $\bar{\Gamma}$. With the initially approximate values of k_D and α_D, the transform of distribution of translational diffusion coefficient to MWD could be conducted by a trial-and-error iteration procedure, and the criterion of the best MWD obtained is that the M_w value calculated from the MWD curve should be in agreement with the experimental M_w value to within a ±8% error limit. As the poly(acrylamide) samples PAM(M) and PAM(S) studied in this work displayed different molecular chain behavior (as mentioned above), the four samples could be categorized into two groups according to their preparation method. The initial approximate values of k_D and α_D for PAM(HM) and PAM(DM) were 1.5×10^{-4} and 0.56, respectively, and the initial values of 3×10^{-4} and 0.56 were, respectively, chosen for k_D and α_D of PAM(HS) and PAM(DS). The last fitting values of k_D and α_D, and M_w, are listed in Table 4. The integral MWD curves are shown in Figure 10a,b. By using a differential computer program, the differential molecular weight distribution curves could be obtained, as shown in Figure 11a,b. It clearly reveals the difference of MWD curves between samples prepared from microemulsion and solution polymerization processes. PAM(M) samples have bimodal MWDs, and higher molecular weights (almost 1 order of magnitude higher) than those polymerized from the solution process PAM(S), which exhibit a one peak MWD; but with a long high molecular weight tail. The lower molecular weights in the solution polymers are due to the chain transfer agent (2-propanol) used.

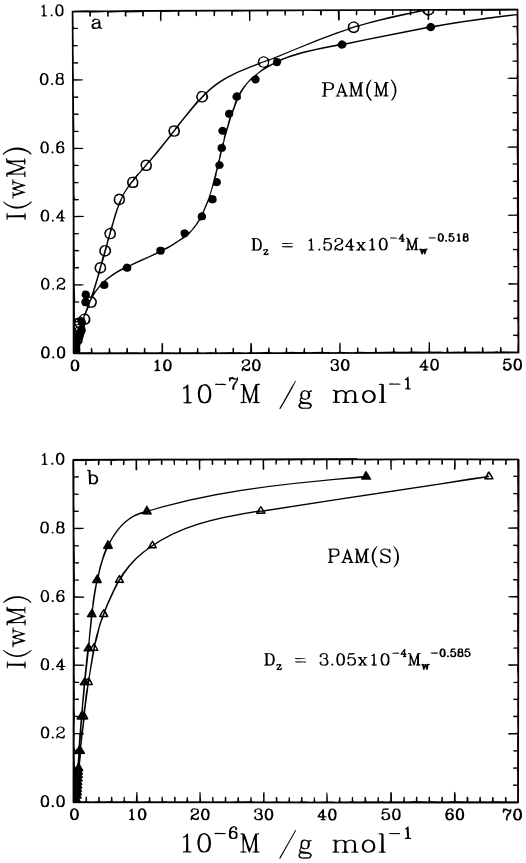

Figure 10. Plot of integral molecular weight distribution of PAM samples. (a) Hollow circles: PAM(HM); full circles: PAM(DM); (b) hollow triangles: PAM(HS); full triangles: PAM(DS).

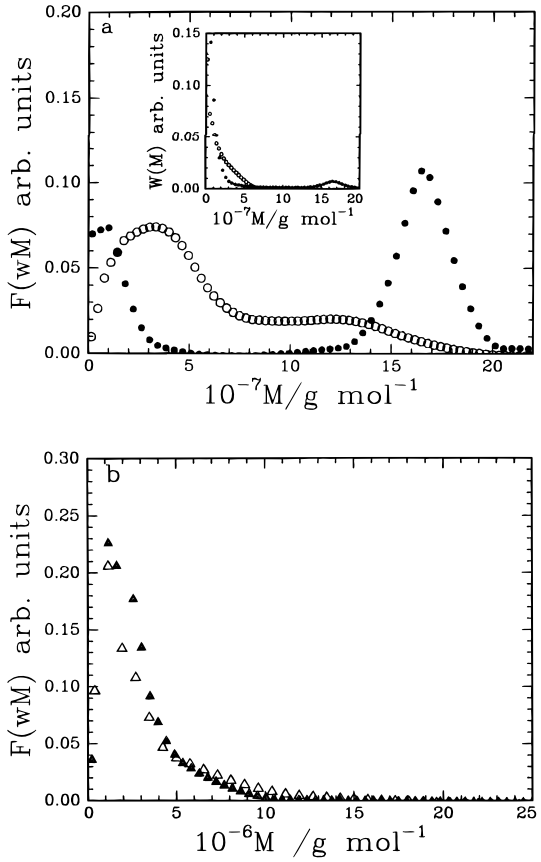

Figure 11. Plot of differential molecular weight distribution ($F(w\mathrm{M})$) of PAM samples. (a) Hollow circles: PAM(HM); full circles: PAM(DM) (inset shows differential weight distribution W(M) of PAM samples); (b) hollow triangles: PAM(HS); full triangles: PAM(DS).

(c) By means of the relationship $R_g = k_g M^{\alpha_g}$, the MWD could be transformed to a radius of gyration distribution (RGD), if k_g and α_g are known. As $R_g \propto R_h$, and $\alpha_g \simeq \alpha_D$. Therefore, for the transformation of MWD to RGD, only one parameter k_g should be considered. The same trial-and-error iteration procedure as performed for the MWD calculation was used for the RGD calculation. The criterion for the best result was that the $\langle R_g \rangle_z$ value calculated from the RGD curve should be in agreement with the experimental R_g value to within a ±5% error limit. In comparison with the experimental results, the fitting parameters are listed in Table 4 and the RGD curves are exhibited in Figure 12a,b. The RGDs of microemulsion polymerized samples show two peaks, as expected.

The R_h values from the experiments designed to compare the behavior of PAM(HM) in 1 M NaCl and in formamide are shown in Table 3, along with those for the linear PAM(SP001). Note that the structural parameter R_g/R_h for PAM(SP001) in 1 M NaCl is the same as for PAM(HS) in Table 1, both falling in the range expected for polydisperse linear chains. For the PAM(SP001) sample in formamide, this parameter remains unchanged, and the apparent M_w is the same as that determined in 1 M NaCl, even though the individual R_g and R_h parameters are different in the two solvents. This attests to the value of the R_g/R_h parameter as a measure of the global chain behavior.

The R_g/R_h parameter for PAM(HM) in 1 M NaCl shown in Table 3 is in excellent agreement with the value reported in Table 1, which was from an independent set of measurements. Both values are suggestive of a nonlinear chain topology. However, when this polymer was dissolved in formamide, the apparent M_w decreased by about a quarter and the R_g/R_h parameter increased to a value consistent with a linear chain topology. This suggests noncovalent aggregates in the 1 M NaCl solution which are absent in the formamide solution.

Conclusion

By combining static and dynamic light scattering, the chain properties, i.e., chain linearity and polydispersity, of PAM in 1 M NaCl aqueous solution were studied. From SLS it can be seen that the PAM(M) synthesized by using a microemulsion process behaved as branched flexible chains, but PAM(S) synthesized from a solution polymerization process exhibited fairly expanded flexible linear coil behavior. CONTIN was used to find the smoothest non-negative intensity distribution consistent with dynamic light scattering data. In combination with static light scattering (SLS), the linewidth distribution was converted to the molecular weight distribution (MWD) and the radius of gyration distribution (RGD). The results show that PAM(M) samples have bimodal MWDs, and higher molecular weights (almost 1 order of magnitude higher) than the PAM(S) polymerized from the solution process. The PAM(S) samples exhibit a unimodal MWD with a long high molecular weight tail.

The origin of the apparent branching in the microemulsion prepared poly(acrylamide) is a noncovalent aggregate which readily dissociates in formamide to yield the constituent linear chains. The aggregates nominally consist of about four linear chains which

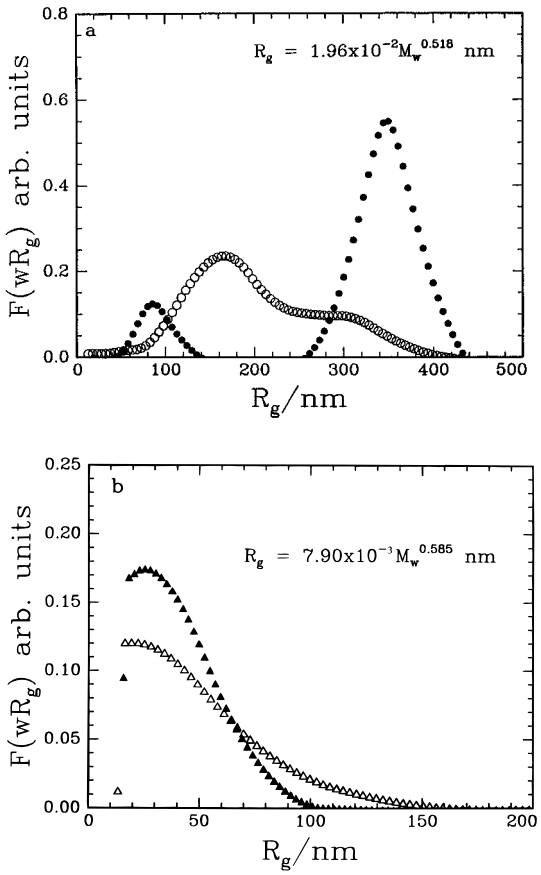

Figure 12. Plot of radius of gyration distribution of PAM samples. (a) Hollow circles: PAM(HM); full circles: PAM-(DM); (b) hollow triangles: PAM(HS); full triangles: PAM-(DS).

form a completely soluble species having a more compact configuration than a linear chain. The presence of these aggregates may be promoted by the polymer isolation procedure, especially the drying stage after precipitation.

Acknowledgment. B.C. gratefully acknowledges support of this work by the National Science Foundation, Polymers Program (DMR 9301294), the Human Frontier Science Program (Strasbourg, France), and the National Center for Human Genome Research (1R0 1HG0138601).

References and Notes

(1) Bode, H. J. *Anal. Biochem.* **1977**, *83*, 364.
(2) de Gennes, P. G. *Scaling Concepts in Polymer Physics*; Cornell University Press: Ithaca, NY, 1979; Chapter 3.
(3) For example, see: Grossman, P. D.; Soane, D. S. *J. Chromatogr.* **1991**, *559*, 257.
(4) Chiari, M.; Nesi, M.; Righetti, P. G. *J. Chromatogr.* **1993**, **A**, *652*, 31.
(5) Holtzscherer, C.; Wittman, J. C.; Guillon, D.; Candau, F. *Polymer* **1990**, *31*, 1978.
(6) Candau, F.; Holtzscherer, C. *J. Chim. Phys.* **1989**, *86*, 2095.
(7) Wang, Z. L.; Chu, B.; Wang, Q.-W.; Fetters, L. In *New Trends in Physics and Physical Chemistry of Polymers*; Lee, L.-H., Ed.; Plenum Publishing Corp.: New York, 1989.
(8) Kulicke, W. M.; Kniewske, R.; Klein, J. *Prog. Polym. Sci.* **1982**, *8*, 373.
(9) *Handbook of Chemistry and Physics*; CRC Press, 1979−1980, D-262.
(10) Ying, Q.-C.; Marecek, J.; Chu, B. *J. Chem. Phys.* **1994**, *101*, 2665.
(11) de Gennes, P. G. *Scaling Concepts in Polymer Physics*; Cornell University Press: Ithaca, NY, 1979; p 78.
(12) Ying, Q.-C.; Qian, R. *Sci. Sin.* **1982**, 961.
(13) Qian, R.; Ying, Q.-C.; Cao, T.; Fetters, L. J. *Kexue Tongbao* **1983**, 354.
(14) Burchard, W. *Macromolecules* **1977**, *10*, 919.
(15) Burchard, W.; Kajiwara, K.; Nerger, D. *J. Polym. Sci., Polym. Phys. Ed.* **1982**, *20*, 157.
(16) Griebel, T.; Kulicke, W. M. *Makromol. Chem.* **1992**, *193*, 811.
(17) Biggs, S.; et al. *J. Phys. Chem.* **1992**, *96*, 1505.
(18) Boyadjian, R.; et al. *Eur. Polym. J.* **1976**, *12*, 401.
(19) Koppel, D. E. *J. Chem. Phys.* **1972**, *57*, 4814.
(20) Chu, B.; Ford, J. R.; Dhadwal, H. S. In *Methods of Enzymolozy*; Collowick, S., Kaplan, N. O., Ed.; Academic: Orlando, 1985; Vol. 117.
(21) Provencher, S. W. *Makromol. Chem.* **1979**, *180*, 201.
(22) Burchard, B.; Schmidt, M.; Stockmayer, W. H. *Macromolecules* **1980**, *13*, 580.
(23) Thurn, A.; Burchard, W.; Niki, R. *Colloid Polym. Sci.* **1987**, *265*, 653.

MA951798N